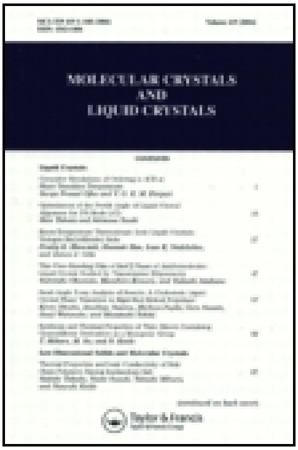

Molecular Crystals and Liquid Crystals
Publication details, including instructions for authors and subscription information:
http://www.tandfonline.com/loi/gmcl20

TD-DFT Studies of Electronic Structures in Cyclometalated Phenylpyrazol Ir(III) Complexes: Fac-Ir$(ppz)_3$ and Ir$(ppz)_2$(acac)

Gyu Choi [a], Jung Lee [a], No Park [b] & Young Kim [c]

[a] Department of Chemical Engineering, Hongik University, Seoul, Korea

[b] Research Institute for Science and Technology, Hongik University, Seoul, Korea

[c] Department of Science, Hongik University, Seoul, Korea

Version of record first published: 18 Oct 2010

To cite this article: Gyu Choi, Jung Lee, No Park & Young Kim (2004): TD-DFT Studies of Electronic Structures in Cyclometalated Phenylpyrazol Ir(III) Complexes: Fac-Ir$(ppz)_3$ and Ir$(ppz)_2$(acac), Molecular Crystals and Liquid Crystals, 424:1, 173-185

To link to this article: http://dx.doi.org/10.1080/15421400490506135

Mol. Cryst. Liq. Cryst., Vol. 424, pp. 173–185, 2004
Copyright © Taylor & Francis Inc.
ISSN: 1542-1406 print/1563-5287 online
DOI: 10.1080/15421400490506135

TD-DFT STUDIES OF ELECTRONIC STRUCTURES IN CYCLOMETALATED PHENYLPYRAZOL Ir(III) COMPLEXES: *fac*-Ir(ppz)$_3$ AND Ir(ppz)$_2$(acac)

Gyu Cheol Choi and Jung Eun Lee
Department of Chemical Engineering, Hongik University,
Seoul, Korea

No Gill Park
Research Institute for Science and Technology, Hongik University,
Seoul, Korea

Young Sik Kim
Department of Science, Hongik University, Seoul, Korea

*The ground state and low-lying excited electronic states of two related Ir(III) complexes fac-Ir(ppz)$_3$ (**1**) and Ir(ppz)$_2$(acac) (**2**) are studied using density functional theory where ppz = phenylpyrazol, acac = acetylacetonate and fac = facial. The complex 1 is a blue phosphorescent material with about 450 nm of electroluminescent peak. The ground states of these complexes are studied using Becke's three parameter hybrid functional with Perdew 86(B3LYP) and the structure analysis of the optimized geometries are processed. Excited triplet and singlet states are examined using time-dependent density functional theory. Every low-lying transition for the former molecule and 6 lowest singlet and triplet excitations for the latter molecule are categorized as metal-to-ligand charge-transfer transitions, because the metal orbitals involved in the transitions have significant admixture of ligand π character with amount of metal 5d character in the occupied molecular orbitals related to those transitions. Through the comparison of the calculated excitons with experimental absorption spectra, each peak was examined its originality.*

Keywords: blue; DFT; Ir complex; Ir(ppz)$_3$; Ir(ppz)$_2$(acac); OLED; phosphorescence

Received 1 October 2003; accepted 14 February 2004.
This work was supported by 2004 Hongik University Research Fund.

Address correspondence to Young Sik Kim, I-dong-309 ho, sang-su-dong 72-1 Mapo-gu, Seoul 121-791, Korea. Tel.: 82-2-320-1670, Fax: 82-2-3142-0335, E-mail: youngkim@hongik.ac.kr

INTRODUCTION

Since Tang and the coworkers reported organic light-emitting devices (OLED) with the multi-layer structure [1], materials for the devices have been extensively studied over the past decade [2]. Luminescent materials for these devices are generally classified into two groups as fluorescent ones and phosphorescent ones. Recently, Forrest and Thompson have developed electrphosphorescent OLEDs with high efficiency approaching 100% of internal quantum efficiency which utilize both singlet and triplet excitons using the phosphorescent dopants [3].

The heavy metal such as Ir or Pt in the complex forms was known to induce the intersystem crossing by strong spin-orbit coupling, leading to mixing of the singlet and triplet excited states [4,5]. Spin-forbidden nature of radiative relaxation from the triplet excited state then becomes allowed, resulting in high phosphorescent efficiencies. Thus, both metal complexes have extensively been introduced to the emitting layers as dopants in OLEDs. In addition, Ir complexes were known to have high photoluminescence efficiency and relatively short excited state lifetime which minimizes quenching of triplet emissive states [6].

In recent years, many approaches using density functional theory (DFT) have received large acceptance for describing the ground state properties of organometallic and inorganic molecules. Especially, using hybrid density functionals [7,8] such as B3LYP and B3PW91, a lot of remarkable structural and thermochemical predictions have been obtained. Also, applications of time-dependent DFT method (TD-DFT) [9,10] which calculated the excited states of molecules have recently begun to be reported on transition metal complexes [12–15], together with Alq_3 [16,17].

Though many phosphorescent materials have been reported in many literatures so far, there have been few reports on pure blue phosphorescent materials whose emission peak is located near 450 nm and luminescent efficiency is high. Recently, we reported the synthesis of $Ir(ppz)_3$ and fabrication of OLEDs where the complex emitted sharp pure blue light with 450 nm [18]. In this paper, we explore the ground and low-lying excited states of molecules (1) and (2) using density functional approaches techniques to understand phosphorescent mechanism. The ground states were treated using the B3LYP functional and the optimized structure was discussed with comparison of ppz ligand. The low-lying triplet and singlet excited states were examined using TD-DFT calculations. The results were compared with absorption spectrum of molecules (1) and (2).

DETAILS OF THE CALCULATIONS

Computationally, the electronic ground states of ppz ligand, the molecules (1) and (2) were calculated using the B3LYP density functional theory. LANL2DZ [19] and 6–31G(d) [20] basis sets were employed for the Ir and other atoms, respectively. To obtain the excitation energy of singlets and triplets time-dependent DFT(TD-DFT) calculations using the B3LYP functional was performed at the respective ground-state geometry, where the basis set of ppz ligands was changed to 6–31 + G(d) for the first excited state calculation of the complex. Typically the lowest 10 triplet and 10 singlet roots of the nonhermitian eigenvalue equations were obtained to get the vertical excitation energies and compared with the absorption spectrum to examine each peaks. The ground-state B3LYP and excited-state TD-DFT calculations were carried out using Gaussian 98 [21].

RESULTS AND DISCUSSION

The results of the optimized structure for the Ir complexes **1** and **2** (Fig. 1) are summarized in Table 1, with those for the ppz ligand and *fac*-Ir(ppy)$_3$

TABLE 1 Comparison of Calculated Bond Lengths for Molecules **1** and **2**, *fac*-Ir(ppy)$_3$ and ppz Ligand

Parameter	ppz	*fac*-Ir(ppz)$_3$	Ir(ppz)$_2$acac	*fac*-Ir(ppy)$_3$* (Å)
Ir-Cl		2.033	2.017	2.035
Ir-Nl		2.169	2.039	2.167
Ir-Ol			2.191	
C1-C2	1.393	1.407	1.403	
C2-C3	1.396	1.397	1.398	
C3-C4	1.395	1.397	1.397	
C4-C5	1.394	1.393	1.394	
C5-C6	1.400	1.396	1.394	
C6-C1	1.400	1.415	1.413	
C6-N2	1.421	1.427	1.423	
N2-C7	1.370	1.358	1.356	
C7-C8	1.377	1.385	1.386	
C8-C9	1.414	1.406	1.409	
C9-N1	1.327	1.335	1.336	
N1-N2	1.360	1.356	1.359	

*Refer to: *J. Phys. Chem. A106*, 1634 (2002).

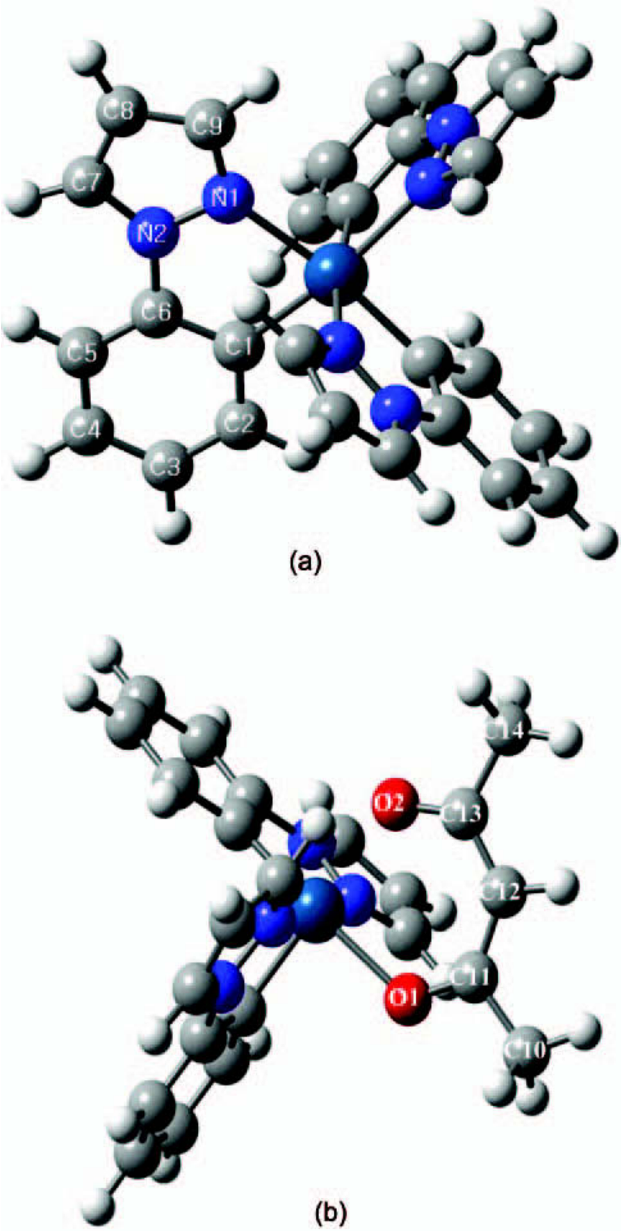

FIGURE 1 Molecular structure of *fac*-Ir(ppz)$_3$ (**1**) and Ir(ppz)$_2$(acac) (**2**).

for comparison. For the molecule **1**, bond lengths of Ir-C1 and Ir-N1 are very similar to those of *fac*-Ir(ppy)$_3$, respectively. So the bonding near Ir atom in both complexes is very similar. To have such bond lengths, the shape of ppz ligand slightly distorted after complexation. The bond lengths of C1-C6 and N1-N2 are contracted and the ones of C1-C2 and N1-C9 are stretched. In the phenyl ring, the C1 atom bonded to Ir metal is only drastically displaced after complexation. However, the pyrazole ring is totally tilted to the Ir metal as about 3.85° with a little atomic distortion, where the atomic displacement of N1 is lesser than that of C1. Thus, it seems that the pyrazole ring is more rigid than the phenyl one in ppz ligand.

In the case of the molecule **2**, bond lengths of Ir-C1, Ir-N1 and Ir-O1 are 2.017 Å, 2.039 Å and 2.191 Å, relatively contracted with respect to those of *fac*-Ir(ppz)$_3$. To induce this contraction, the angles of N1-N2-C6 and N2-C6-C1 are more leaned to about 1° than those of *fac*-Ir(ppz)$_3$. Change of atomic bond lengths from the ppz ligand to the complex **2** does not shown drastically in comparison with data to **1**. From the calculation of Mulliken charge which gives the quantity of charge localized at each atom, it is possible to find the origin of the contraction between Ir and nearest atoms. The charges of central Ir atom are 0.790 for the molecule **1** and 0.99 for then molecule **2**. And, those of C1 and N1 which are most closely located near Ir atom are –0.19 and –0.25 for the prior molecule and –0.22 and –0.33 for the last one. For the case of oxygen atom in acac ligand of the molecule **2**, the value is more bigger to –0.49. Thus, it would be thought that the strong electronegativity of oxygen atom, which induces the deepening of charge separation between Ir atom and nearest organic atom, result in making those bonds be shorten.

After optimization of molecular structures of ppz ligand, molecules **1** and **2** using density functional theory, energy levels and molecular orbitals were investigated. The results of calculations are shown in Figure 2 and summarized in Table 2. In Table 2, the value of d means that electronic population of any electron localized to centric Ir atom which is a criterion of d character of the orbital. It will be useful to examine the highest occupied molecular orbital (HOMO) and the lowest unoccupied molecular orbital (LUMO), to understand the electronic nature of this Ir complex and to provide the framework for the excited state through TD-DFT calculation. In Table 2, each orbitals are labeled following Hey's notation like d_1, d_2, π_1, π_2, etc., where d means that the related molecular orbital(MO) has the character of the metallic d orbital and the electronic population confined to d orbital is more than about 30% [15].

In the case of molecule **1**, only three highest molecular orbitals have the d characters. The strong mixing of d orbitals with π orbitals of ppz ligand is shown on the highest three occupied orbitals, as shown in Figure 3(a)–(c). As a result of strong mixing, the electrons became to be mainly localized to

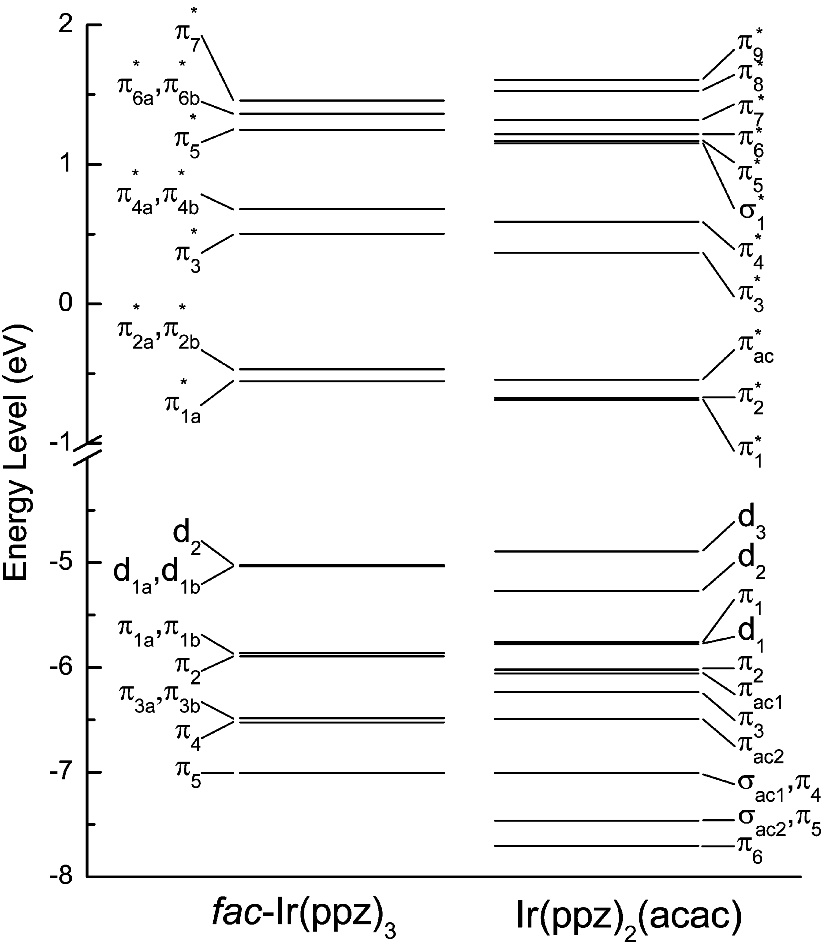

FIGURE 2 Schematic drawing of orbital energies of highest occupied and lowest unoccupied MOs of molecules **1** and **2**.

near the centric metal atom through the bond of Ir and C1 atom in those orbitals. It is also ascertained from the investigation of distribution of orbital in those MOs that the electronic distribution is nearly localized in the phenyl ring except Ir(III) 5d orbitals although it had been delocalized through all the ligand before complexation, as shown in Figure 3(a)–(c). In the case of virtual MOs of this complex, there is no any proof about strong mixing between 5d and π orbitals. The calculated electronic populations localized centric Ir metal are very small in every virtual MOs

TABLE 2 Calculated Occupied and Virtual Orbital Energies of Molecules **1** and **2**

Occupied molecular orbitals					Unoccupied molecular orbitals				
No		Symm.	Energy (eV)	d(%)	No		Symm.	Energy (eV)	d(%)
(a) *fac*-Ir(ppz)3									
121	d_2	41a	–5.025	50.2	122	$\pi_1{}^*$	42a	–0.554	0.1
120	d_{1a}	80e	–5.037	47.8	123	$\pi_{2a}{}^*$	81e	–0.471	3.2
119	d_{1b}	79e	–5.037	47.8	124	$\pi_{2b}{}^*$	82e	–0.471	3.2
118	π_{1a}	78e	–5.864	8.1	125	$\pi_3{}^*$	43a	0.502	0.7
117	π_{1b}	77e	–5.864	8.1	126	$\pi_{4a}{}^*$	83e	0.679	5.3
116	π_2	40a	–5.898	10.7	127	$\pi_{4b}{}^*$	84e	0.679	5.3
115	π_{3a}	76e	–6.487	17.5	128	$\pi_5{}^*$	44a	1.248	1.4
114	π_{3b}	75e	–6.487	17.5	129	$\pi_{6a}{}^*$	85e	1.363	2.0
113	π_4	39a	–6.527	21.1	130	π_{6b}	86e	1.363	2.0
112	π_5	38a	–7.011	4.0	131	π_7	45a	1.456	0.2

Occupied molecular orbitals				Unoccupied molecular orbitals			
No		Energy (eV)	d(%)	No		Energy (eV)	d(%)
(b) Ir(ppz)2acac							
110	d_3	–4.895	49.9	111	$\pi_1{}^*$	–0.689	2.7
109	d_2	–5.270	37.1	112	$\pi_2{}^*$	–0.673	2.1
108	π_1	–5.757	0.3	113	$\pi_{ac}{}^*$	–0.542	2.1
107	d_1	–5.780	65.7	114	$\pi_3{}^*$	0.367	4.8
106	π_2	–6.021	5.5	115	$\pi_4{}^*$	0.587	10.1
105	π_{ac}	–6.057	27.0	116	$\sigma_1{}^*$	1.148	28.6
104	π_3	–6.237	27.0	117	$\pi_5{}^*$	1.167	0.9
103	π_{ac}	–6.493	20.6	118	$\pi_6{}^*$	1.217	1.2
102	σ_{ac},π_4	–7.008	3.1	119	$\pi_7{}^*$	1.316	10.8
101	σ_{ac},π_5	–7.465	7.2	120	$\pi_8{}^*$	1.527	0.3
100	π_6	–7.705	21.5	121	$\pi_9{}^*$	1.606	1.8

calculated in this study. More precise descriptions on the complex **1** were written our previous paper [22].

In the case of the complex **2**, two highest MOs are evidently shown to be strongly mixed between d orbital of centric Ir metal and π orbital of ppz ligand, whose electronic populations are 49.9% and 37.1% respectively. These are lesser than those of $Ir(ppy)_2(acac)$, which are 67% and 45% [15]. The HOMO-2 in Figure 3(i) shows seriously different character in orbital distribution which has only π character localized in ligand, similar shape of the HOMO-1 of the ppz ligand. On the contrary, Hay reported that the HOMO-2 of $Ir(ppy)_2(acac)$ was also strongly mixed between d and π orbitals.

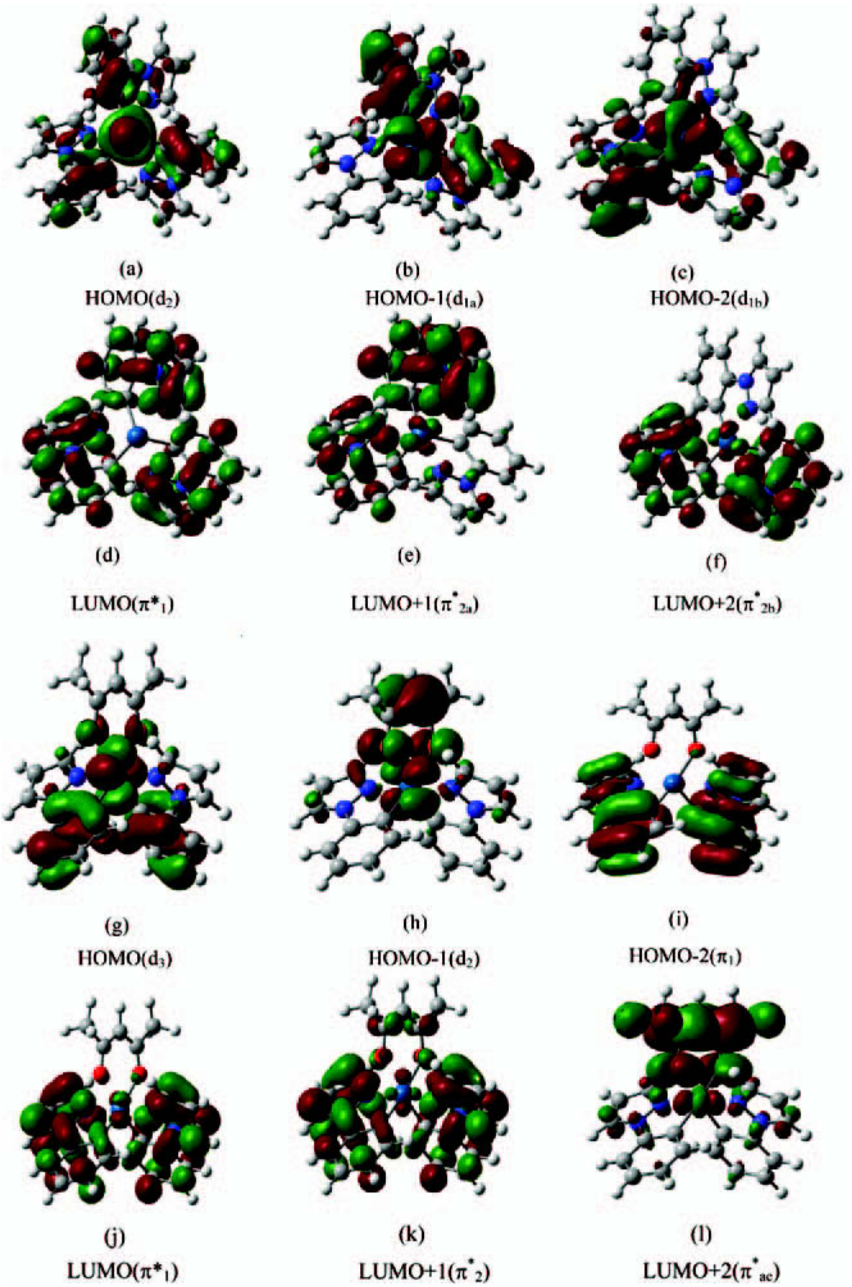

FIGURE 3 Contour plots of HOMOs and LUMOs. (a) ∼ (f) for molecule **1,** and (g) ∼ (l) for molecules **2**.

In the case of Ir(ppy)$_2$(acac), this orbital is deeply embedded. This orbital take a key role of red-shift that absorption and emission peaks are bathochromically changed, which will be described later. And, separations between MOs are rather bigger. This is thought to be change of symmetry to C1.

In the HOMO of the molecule **2**, mixing trend is slightly different from that of molecule **1** while HOMO-1 and HOMO-3 are similar. Predominant difference is that the symmetry axis of d orbital in HOMO follows the direction located prior to complexation, notwithstanding that the axes of d orbitals of HOMO-1 and HOMO-3 follow center of prior three axes like the case of the molecule **1**. Only in a geometrical view point, it would be thinkable that any position of three orthogonal axes is more stable than that of two orthogonal ones. So, the HOMO is located higher and the separation of energy levels is wider than those of the molecule **1**.

In the case of virtual MOs of the molecule **2**, two lowest virtual MOs have only π character of ppz ligand without any d character, and the third virtual MO is related to the acac ligand. Accordingly, HOMO and LUMO of acac ligand are inserted among the MOs induced from ppz ligand after complexation. Other higher virtual MOs also show π character of ppz ligand except a MO having σ character which is slightly mixed with d orbital of Ir metal with 28% of d character. Hence, provided that any transition occurs from two highest HOMO or HOMO-3 to any MO of 10 lowest ones, the transition would be possible to be called as metal-to-ligand charge transfer (MLCT).

TD-DFT calculation was employed to examine the low-lying singlet and triplet states of the complexes and results are shown in the Table 3. For the molecules **1** and **2**, we typically give the vertical excitation energies for the lowest ten triplet and singlet states calculated at the optimized structure for the ground states. For each of triplet and singlet excitations, a dominant excitation is achieved among several minor excitations, present because of strong d-π mixing, if its transition probability is the greatest one. Even though, for the triplet cases, there still exist many transition states having same excitation energy than those for the singlet ones. In the case of the molecule **1** as shown in Table 3, we see the lowest triplet states (T_1) is 3.14 eV with two higher triplet states extremely close within 0.01 eV in energy. This characteristic is very similar with that of *fac*-Ir(ppy)$_3$ with only a difference of excitation energy. All correspond to excitations from an electron in the three highest occupied MOs with the significant 5d character to virtual MOs with π^* character. According to this assessment, it is certain that every excitations calculated in this study are MLCT states.

For the complex **2**, the lowest triplet excitation energy is 2.93 eV which is 0.45 eV less than that of Singlet excition. Here, the origin of those excitions is considerably different. In the singlet case, the lowest excitation S_1 is due to the transition from HOMO to LUMO in similar with lowest excitations of

TABLE 3 Calculated Excitation Energies, Dominant Orbital Excitation, and Oscillator Strengths Obtained from TD-DFT Calculations for Molecules **1** and **2**

Singlets					Triplets			
States	Dominant excitation	Energy (eV)	Wave-length (nm)	Oscillator Strengths	States	Dominant excitation	Energy (eV)	Wave-Length (nm)
(a) fac-Ir(ppz)3								
$S_1(^1A)$	$d_2 \rightarrow \pi_1{}^*$	3.56	348.1	0.0141	$T_1(^3A)$	$d_2 \rightarrow \pi_1{}^*$	3.14	394.5
$S_2(^1E)$	$d_{1b} \rightarrow \pi_1{}^*$	3.62	342.1	0.0275	$T_2(^3E)$	$d_{1a} \rightarrow \pi_1{}^*$	3.15	394.3
	$d_{1a} \rightarrow \pi_1{}^*$	3.62	342.1	0.0277		$d_{1b} \rightarrow \pi_1{}^*$	3.15	394.3
$S_3(^1E)$	$d_2 \rightarrow \pi_{2a}{}^*$	3.66	338.8	0.0053	$T_3(^3A)$	$d_2 \rightarrow \pi_1{}^*$	3.43	361.4
	$d_2 \rightarrow \pi_{2b}{}^*$	3.66	338.8	0.0052				
					$T_4(^3E)$	$d_2 \rightarrow \pi_{2a}{}^*$	3.45	359.2
						$d_2 \rightarrow \pi_{2a}{}^*$	3.45	359.2
$S_4(^1A)$	$d_{1a,1b} \rightarrow \pi_{2a,2b}{}^*$	3.70	335.5	0.0039				
$S_5(^1A)$	$d_{1a,1b} \rightarrow \pi_{2a,2b}{}^*$	3.76	329.9	0.0556	$T_5(^3A)$	$d_2 \rightarrow \pi_1{}^*$	3.58	345.7
	$d_{1a,1b} \rightarrow \pi_{2a,2b}{}^*$	3.76	329.9	0.0556				
					$T_6(^3E)$	$d_{1a} \rightarrow \pi_1{}^*, d_2 \rightarrow \pi_{2a}{}^*$	3.59	345.3
						$d_{1b} \rightarrow \pi_1{}^*, d_2 \rightarrow \pi_{2b}{}^*$	3.59	345.3
$S_6(^1A)$	$d_{1a,1b} \rightarrow \pi_{2a,2b}{}^*$	3.85	322.2	0.0622				
$S_7(^1A)$	$d_2 \rightarrow \pi_{4a}{}^*$	4.56	271.8	0.0090	$T_7(^3A)$	$d_2 \rightarrow \pi_{2a}{}^*$, $d_{1b} \rightarrow \pi_1{}^*$	3.64	340.2
(b) Ir(ppz)2acac								
S_1	$d_3 \rightarrow \pi_1{}^*$	3.38	366.3	0.0353	T_1	$d_2 \rightarrow \pi_{ac}{}^*$	2.93	423.7
S_2	$d_3 \rightarrow \pi_2{}^*$	3.40	364.1	0.0012	T_2	$d_3 \rightarrow \pi_1{}^*$	3.07	403.8
S_3	$d_3 \rightarrow \pi_{ac}{}^*$	3.46	358.6	0.000	T_3	$d_3 \rightarrow \pi_2{}^*$	3.09	401.2
S_4	$d_3 \rightarrow \pi_2{}^*$	3.80	326.2	0.0378	T_4	$d_3 \rightarrow \pi_{ac}{}^*$	3.36	369.3
S_5	$d_2 \rightarrow \pi_1{}^*$	3.81	325.0	0.008	T_5	$d_2 \rightarrow \pi_1{}^*$	3.48	356.0
S_6	$d_2 \rightarrow \pi_{ac}{}^*$	3.93	315.7	0.0122	T_6	$d_2 \rightarrow \pi_2{}^*$	3.50	354.4
S_7	$\pi_1 \rightarrow \pi_2{}^*$	4.21	294.3	0.0227	T_7	$\pi_2 \rightarrow \pi_2{}^*$ $d_1 \rightarrow \pi_1{}^*$	3.59	345.1
S_8	$\pi_1 \rightarrow \pi_1{}^*$	4.21	294.2	0.0595	T_8	$\pi_2 \rightarrow \pi_1{}^*$	3.59	345.1
S_9	$\pi_1 \rightarrow \pi_{ac}{}^*$	4.35	284.7	0.0308	T_9	$\pi_1 \rightarrow \pi_1{}^*$	3.89	318.4
S_{10}	$d_3 \rightarrow \pi_3{}^*$	4.46	277.7	0.0322	T_{10}	$\pi_1 \rightarrow \pi_2{}^*$	3.91	317.0

fac-Ir(ppy)$_3$ and Ir(ppy)$_2$(acac). However, the triplet excitation is the transition HOMO-1 to LUMO + 2 which is an extraordinary case. The electron population of d character in HOMO-1 is 37.1% which is slightly small in comparion with those of *fac*-Ir(ppy)$_3$ and Ir(ppy)$_2$(acac). It means that the d-π mixing is relatively weak in the MO. And the excitation would be occur from a weakly d-π mixed occupied orbital to a virtual orbital localized at acac ligand not ppz ligand, a kind of MLCT transition. As a result, the absorption and emission peaks would be bathochromically shifted and the emissive color of PL or EL would be greenish blue in the region of 470 ~ 480 nm.

For the comparison with experimental data, we plotted the results obtained through the TD-DFT in the absorption spectra of the molecues **1** and **2**, as shown in Figure 4. For the case of **1**, it is certain that peaks distributed from 280 nm to 410 nm would be assigned to MLCT absorptions that singlets ($S_1 \sim S_7$) and triplets ($T_1 \sim T_7$) are separately located in the region of 270 nm ~ 350 nm and 340 nm ~ 410 nm, respectively. Especially, the peak located at about 325 nm is due to S_5 and S_6 whose oscillator strengths are dominant. Triplets T_1, T_5 and T_6 are originated to same transition with that of S_1. It is thought to be the result of configuration interaction.

For the case of the complex 2, three distinct regions in absorption spectrum exists. At first, in the region of 354 nm ~ 423 nm, the absorbance is originated to ^{3}MLCT. In the region of 350 nm ~ 300 nm, ^{3}LC and ^{1}MLCT are coexists. At last, there exists ^{1}LC in the region less than 300 nm. In the energy diagram of singlet and triplet excitation, the T_1 has similar transition mechanism with S_6 which induces the redish shift of absorption and emission spectrum to about 30 nm. The reason of energy decreasing of T_1 triplet is still unclear and it is thought that more study is needed.

CONCLUSION

The ground state and low-lying excited electronic states in the Ir(III) complex **1** and **2** are studied using density functional theory. The electronic properties of the molecule are calculated using the B3LYP functional. The structure analysis of the optimized geometries are processed in comparison with structures of ppz ligand, *fac*-Ir(ppy)$_3$, and Ir(ppy)$_2$(acac) which already reported before. Excited triplet and singlet states are examined using TD-DFT. The calculated energies of the lowest triplet and singlet states are 3.14 eV and 3.56 eV for the molecule **1** and 2.93 eV and 3.38 eV for the molecule. All of the low-lying transitions calculated in this study are categorized as MLCT transitions for molecule **1** because the metal 5d character of three highest MOs which are 50.2%, 47.8% and 47.8%, respectively. However, for the molecule **2**, 6 lower triplets and singlets

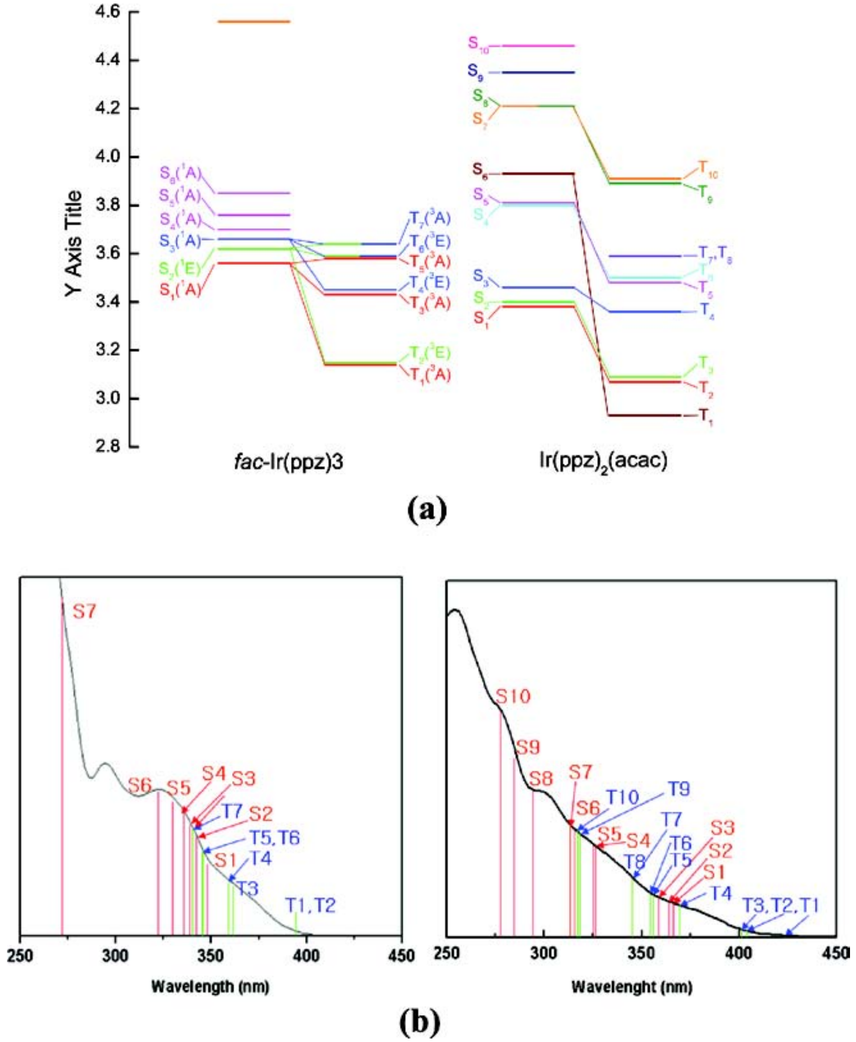

FIGURE 4 (a) Schematic energy levels of excited states and (b) UV/VIS absorption spectrum of molecules **1** and **2**.

are categorized as MLCT transitions and other higher states are branched to LC transitions. From the analysis of absorption spectrum of this complex, it was found that the calculated singlets and triplets were distributed in the range of 270 nm∼350 nm and 340 nm∼410 nm in absorption spectrum for the former molecule and in the range of 280 nm∼370 nm and 320 nm∼420 nm for the latter, rather widely.

REFERENCES

[1] Tang, C. W. & Van Slyke, S. A. (1987). *Appl. Phys. Lett., 51*, 913.

[2] Tang, C. W. (1996). Informatin display *10*, 16; Hamada, Y. (1997). *IEEE Trans. On Electron. Dev., 44*, 1208; Chen, C. H. & Shi, J. (1998). *Coord. Chem. Rev., 171*, 161.

[3] Baldo, M. A., Thompson, M. E., & Forrest, S. R. (2000). *Nature, 403*, 750.

[4] Lamansky, S., Djurovich, P., Murphy, D., Abdel-Razzaq, F., Lee, H.-E., Adachi, C., Burrows, P. E., Forrest, S. R., & Thompson, M. E. (2001). *J. Am. Chem. Soc., 123*, 4304; Lamansky, S., Djurovich, P., Murphy, D., Abdel-Razzaq, F., Kwong, R., Tsyba, I., Bortz, M., Mui, B., Bau, R., & Thompson, M. E. (2001). *Inorg. Chem., 40*, 1704; Tsutsui, T., Yang, M.-J., Yahiro, M., Nakamura, K., Watanabe, T., Tsuji, T., Fukuda, Y., Wakimoto, T., & Miyaguchi, S. (1999). *Jpn. J. Appl. Phys., 38*, L1502.

[5] Baldo, M. A., Thompson, M. E., & Forrest, S. R. (1999). *Pure Appl. Chem., 71*, 2095; Chan, S.-C., Wang, Y., Che, C.-M., Cheung, K.-K., & Zhu, N. (2001). *Chem. Eur. J., 19*, 4180; Brooks, J., Babaya, Y., Lamansky, S., Djurovich, P. I., Tsyba, I., Bau, R., & Thompson, M. E. (2002). *Inorg. Chem. 41*, 3055.

[6] Dedeian, K., Djurovich, P. I., Carlson, F. O., & Watts, R. J. (1991). *Inorg. Chem., 30*, 1685.

[7] Lee, C., Yang, W., & Parr, R. G. (1988). *Phys. Rev., B37*, 785.

[8] Becke, A. D. (1993). *J. Chem. Phys., 98*, 5648.

[9] Jamorski, C., Casida, M. E., & Salahub, D. R. (1996). *J. Chem. Phys., 104*, 5134.

[10] Petersilka, M., Grossmann, U. J., & Gross, E. K. U. (1996). *Phys. Rev. Lett., 76*, 1212.

[11] Stratmann, R. E., Scuseria, G. E., & Frisch, M. J. (1998). *J. Chem. Phys., 109*, 8218.

[12] Rosa, A., Baerends, E. J., vanGisbergen, S. J. A., vanLenthe, E., Gooeneveld, J. A., & Snijders, J. G. (1999). *J. Am. Chem. Soc., 121*, 10356.

[13] Adamo, C. & Barone, V. (2000). *Theo. Chem. Acc., 105*, 169.

[14] Farrell, I. R., van Slageren, J., Zalis, S., & Vlcek, A. (2001). *Inorg. Chim. Acta, 315*, 44.

[15] Hay, P. J. (2002). *J. Phys. Chem., A106*, 1634.

[16] Martin, R. L., Kress, J. D., Campbell, I. H., & Smith, D. L. (2000). *Phys. Rev., B61*, 15804.

[17] Halls, M. D. & Schelgel, H. B. (2001). *Chem. Mater., 13*, 2632.

[18] Nam, E. J., Kim, J. H., Kim, B. O., Kim, S. M., Park, N. G., Kim, Y. S., Kim Y. K., & Ha, Y. *Bull. Chem. Soc. Jap.*, submitted.

[19] Hay, P. J. & Wadt, W. R. (1985). *J. Chem. Phys., 82*, 270; *ibid*. 284; *ibid*. 299.

[20] Hehre, W. J., Ditchfield R., & Pople, J. A. (1972). *J. Chem. Phys., 56*, 2257.

[21] Frisch, M. J. *et al.* (1988). Gaussian 98, revision A.9, Gaussian, Inc., Pittsburgh, PA.

[22] Park, N. G., Choi, G. C., Lee, J. E., & Kim, Y. S. *Curr. Appl. Phys.,* submitted.